Journal of Thermal Analysis and Calorimetry (2020) 139:319–331
https://doi.org/10.1007/s10973-019-08413-3

The effect of polymer dispersions on the early hydration of calcium sulfoaluminate cement

Lin Li[1] · Yu Peng[2] · Ru Wang[1,3] · Shaokang Zhang[1]

Received: 29 January 2019 / Accepted: 24 May 2019 / Published online: 4 June 2019

Abstract

The influence of three polymer dispersions [styrene–butadiene copolymer (SB), styrene–acrylic ester copolymer (SA) and polyacrylic ester (PA)] on the hydration of calcium sulfoaluminate (CSA) cement within 72 h was investigated by using isothermal conduction calorimetry, X-ray diffraction analysis and thermal gravimetric analysis. The results indicate that these three polymer dispersions perform different influences on the hydration heat flow of CSA cement during different periods, they all postpone the occurrence time of the maxima peaks, and its extent is mainly dependent on the addition amount. Polymer dispersions manifest great retardation on the initial hydration of CSA cement, and the effect is much more significant within 1 h. In this stage, the generation of ettringite is strongly delayed; however, the formation of ettringite is accelerated by these polymer dispersions at and after 2 h. Among these three polymer dispersions, PA demonstrates the highest acceleration effect on the hydration degree.

Keywords Calcium sulfoaluminate cement · Polymer dispersions · Hydration · Calorimetry

Introduction

Polymer-modified cement mortar and concrete have been widely used as popular construction materials in the world since the concept of polymer modification for cement mortar and concrete was put forward before 80 years [1]. Polymer admixtures, especially polymer dispersions, are formulated into cement mixtures for modification of cement mortar and concrete. The key properties of polymer dispersions are their ability to form flexible and homogeneous polymer films inside of cement matrix along with the cement hydration process [2, 3], which gives cement mortar and concrete well adhesion and cohesion properties [4]. The use of these dispersions in cementitious materials contributes to decrease water-to-cement ratio [5], increase strength and improve durability [6–11]. The formed 3D polymer films within cement matrix would also benefit to decrease porosity [12] and water absorption [8].

The effect of polymer dispersions on the hydration of Portland cement has been well disclosed from previous studies [13–20]. Generally, the addition of polymer dispersions would retard the hydration of ordinary Portland cement (OPC) [20–30], and this retardation effect becomes much more significant when the bigger polymer content was dosed [31, 32]. It has been widely accepted that its retardation effect is mainly attributed to their adsorption onto the surface of the cement grains and their complexing effects with Ca^{2+} [14, 17]. The negatively charged polymer dispersions can be attracted by cement grains surface with heterogeneous charge distribution, driven by the electrostatic force. The adsorbed polymer layer will hinder the cement hydration by acting as a diffusion barrier layer to suppress the diffusion of water and ions between the mineral phase and aqueous phase [14, 23], thus prolong the induction period and decrease the hydration rate [31]. Meanwhile, the addition of polymer dispersions in cementitious system could decrease the concentration of

✉ Ru Wang
ruwang@tongji.edu.cn

[1] School of Materials Science and Engineering, Tongji University, Shanghai 201804, People's Republic of China

[2] College of Engineering and Architecture, Zhejiang University, Hangzhou 310058, Zhejiang, People's Republic of China

[3] Key Laboratory of Advanced Civil Engineering Materials (Tongji University), Ministry of Education, Shanghai 201804, People's Republic of China

Table 1 Chemical composition of CSA cement/mass%

Al_2O_3	CaO	SO_3	SiO_2	Fe_2O_3	K_2O	MgO	Mn_2O_3	Na_2O	P_2O_5	SrO	TiO_2	Loss on ignition
24.50	44.6	14.89	9.85	2.35	0.31	2.39	0.02	0.08	0.13	0.10	1.00	1.70

Table 2 Mineral composition of CSA cement/mass%

$C_4A_3\bar{S}$	C_2S	$C\bar{S}$	C_4AF	$C_{12}A_7$	CT	$CaMg(CO_3)_2$	MgO
35.9	25.2	21.4	0.6	2.0	12.9	0.9	1.1

free Ca^{2+} in cement pore solution through complexation effect between polymers and Ca^{2+}, thus, the nucleation rate of calcium silicate hydrates (C–S–H) and the precipitation rate of Portlandite are retarded, and finally, the induction period can be prolonged [14, 33]. Lu et al. [14] found that the hydrolysis of ester groups in acrylate units in SA copolymer is significantly accelerated by elevated temperature in alkaline condition. Meanwhile, the continuous production of carboxyl groups promotes the adsorption of polymer particles on the surface of cement grains and/or leads to continuous Ca^{2+} sequestration from pore solution, while finally causes the super-retardation effect on cement hydration [34]. It has been also confirmed that different types of polymer dispersions as well as different functional groups usually perform different retardation effects due to their surface characteristics. Fan et al. [17] investigated the effect of SB copolymer modified with two different chemical groups (carboxyl and sulfonate groups) on the hydration of Portland cement, he found that the adsorption capability of carboxyl groups is higher than that of sulfonate groups, and thus, SB copolymer with carboxyl groups exhibits a stronger retardation effect than that with sulfonate groups. Lu et al. [14] found that the retardation effect of SA-modified cement can be minimized by introducing polyethylene oxide hairy layer on the surface of colloidal particles [34]. Although the retardation effect of polymer dispersions on the Portland cement has been well verified, its influence on the hydrates was not well reported. Wang et al. [19, 35, 36] found that SB accelerates the reaction of calcium aluminate (C_3A) with gypsum in the initial stage and thus enhances the formation and stability of ettringite but inhibits the formation of C_4AH_{13} and $Ca(OH)_2$.

The previous studies regarding to the properties and hydration of polymer-modified cementitious materials mainly focused on OPC, and little is known on the polymer modification of calcium sulfoaluminate (CSA) cement. CSA cement was developed by China Building Materials Academy in the 1970s [37], and it has drawn a great interest from both researchers and industries due to its environmental benefits and technical advantages [38–41]. CSA cement can be produced by burning mixtures of bauxite, limestone and gypsum at around 1250 °C [42]. Its main mineral compositions are ye'elimite ($C_4A_3\bar{S}$), belite (C_2S) and some other minor phases [43–45]. Once it is contacted with water, ettringite (AFt) together with aluminum hydroxide (AH_3) will be formed when calcium sulfate is present while monosulphoaluminate (AFm) is produced when calcium sulfate is completely depleted [46–49]. Furthermore, some other hydration products including hemicarboaluminate (Hc), monocarboaluminate (Mc) or stratlingite can be occurred depending on minor phases presented in the formulation [50, 51].

In this study, the effect of polymer dispersions on the early hydration of CSA cement was investigated. Three widely used polymer dispersions and one typical Chinese CSA cement were taken as raw materials for further analysis. Pastes with five different ratios (0, 5, 10, 15 and 20%) of each polymer dispersion to CSA cement at a constant water-to-cement ratio of 0.4 were investigated.

Experimental

Materials

One Chinese CSA cement was investigated for all experiments. The chemical composition of the used CSA cement determined by X-ray fluorescence is given in Table 1. Its mineral composition quantified by XRD Rietveld method is shown in Table 2. Three different types of polymer dispersions used in the experiment are SB, SA and PA copolymer dispersions, and their physical properties are illustrated in Table 3. The FTIR spectra of three polymer dispersions are displayed in Fig. 1. Figure 2 exhibits the particle size distribution of CSA cement and polymer dispersions. The deionized water was used for the preparation of polymer-modified CSA cement paste.

Test methods

Five different polymer-to-cement ratios by mass (0, 5, 10, 15 and 20%) were considered and water-to-cement ratio of

Table 3 Characteristics of polymer dispersions

		SB dispersion	SA dispersion	PA dispersion
Solid content	%	51 ± 1	57 ± 1	47 ± 1
pH	–	7.0–9.0	7.0–8.5	8.5–10.5
Viscosity (23 °C)	mPa s	50–300	300–750	100–200
Density	g cm^{-3}	~ 1.04	~ 1.04	~ 1.04
Glass transition temperature	°C	+ 14	− 8	+ 12

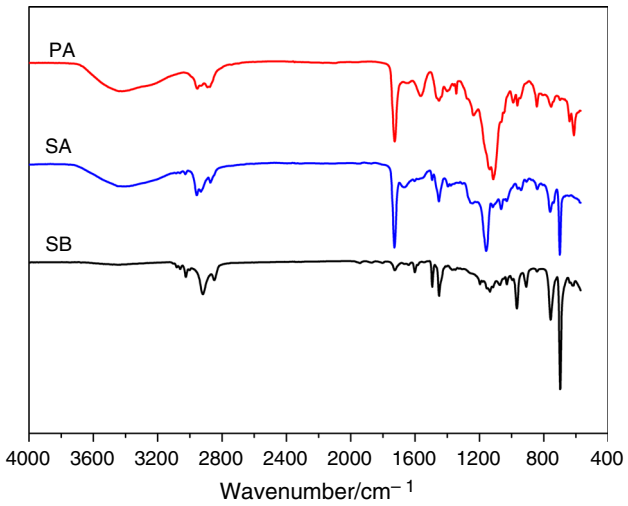

Fig. 1 FTIR spectrum of polymer dispersions

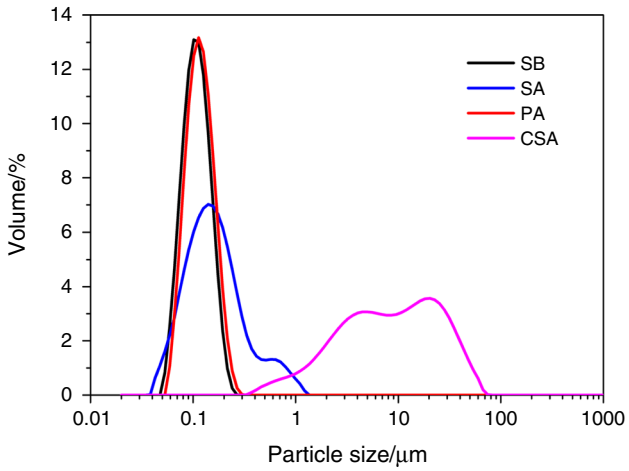

Fig. 2 Particle size distribution of CSA cement and polymer dispersions

0.4 was used to monitor the hydration process of CSA cement modified with various polymer dispersions in all experiments. The polymer dispersion was mixed into water firstly; afterward, a certain mass of CSA cement was weighed into the liquid for the following measurement.

An eight-channel isothermal conduction calorimeter (TAM Air microcalorimeter from TA Instruments) was employed to determine the hydration heat flow at 20 °C within 72 h. 5.00 g of CSA cement was weighed into a specific glass bottle provided by TA Instruments, and the corresponding amount of water and polymer dispersion was added. The paste was mixed 1 min by using a small stirrer with a constant mixing speed at 600 r/min and then transferred into the instrument quickly. Because of the external mixing, the very early thermal response of the samples was omitted. The total heat of hydration within 72 h was determined by integration of the heat flow curve between 20 min and 72 h.

Fresh cement pastes for the following setting time measurement and hydration analysis were mixed 2 min in Hobart mixer. The setting time of polymer dispersion-modified CSA cement mortar was determined according to ISO 9597: 2008 [52] by the use of automatic Vicat apparatus. About 100 g of each fresh paste was sealed in polyethylene bottle, which was immediately moved into environmental chamber for curing at 20 °C. Specimens were then taken to stop hydration by using high-purity ethanol and then ground at the required ages. The analysis samples were further collected after sieving at 100 μm for XRD and TG analysis. XRD measurement was conducted by the use of Rigaku equipment (model D/max2550VB3 +) operating at 40 kV and 250 mA. The step scanning was performed in a range of 5°–60° with a 2θ increment 0.02° every step, a dwell time of 4 s and a Cu Kα radiation. TG test was carried out by using Netzsch TGA 209F1; sample of 20 mg was heated with heating rate of 10 °C min^{-1} from 30 to 950 °C under nitrogen atmosphere.

Results and discussion

Calorimetry analysis

The hydration heat evaluation of CSA cement paste modified with SB dispersion is shown in Fig. 3. The control CSA cement paste displays three main maxima peaks in the heat flow curve as shown in Fig. 3a. The initial one, which occurs in the first minutes, is characterized by the ions dissolution due to the fast reactions upon wetting between

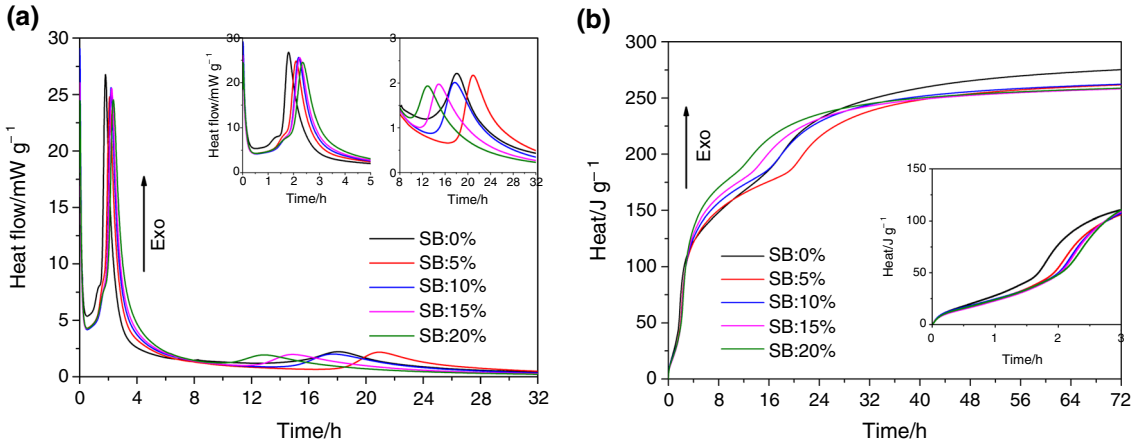

Fig. 3 Hydration heat characteristics of CSA cement pastes modified with SB dispersion: **a** heat flow and **b** cumulative heat

the active phases and water [42, 53–55]. An induction period will occur with relative low heat flow rate. It can be assumed by the coverage of the initial hydration products on the surface of cement grains, which delays the further hydration reaction. Afterward, the hydration heat flow increases and the second peak with very intense and sharp curve is seen at 108 min, which is due to the hydration of the main clinker phases of ye'elimite and calcium sulfate according to Eq. (1). In the literature [42], the main hydration heat peak occurs at 15 h, which is mainly due to the hydration of pure ye'elimite phase in accordance with Eq. (2). When calcium sulfate is present, the hydration of ye'elimite is accelerated; accordingly, the maxima peak occurs in a shorter time although the extent is mainly dependent on the source of calcium sulfate. After reaching the second maximum, the hydration heat flow starts to decline due to the coverage of cement grains by hydration products. This stage undergoes a long time before the last heat peak happens. The third hydration heat peak happens at around 18 h which is attributed to the rapid dissolution of ye'elimite and the formation of a large amount of hydrates (including AFt, AFm and AH_3); then, the formation of ettringite tends to be stable [56, 57].

$$C_4A_3\bar{S} + 2C\bar{S} + 38H \rightarrow C_3A \cdot 3C\bar{S} \cdot 32H + 2AH_3 \quad (1)$$

$$C_4A_3\bar{S} + 18H \rightarrow C_3A \cdot C\bar{S} \cdot 12H + 2AH_3 \quad (2)$$

SB-modified CSA cement pastes show the same trend of hydration heat flow as control paste. However, the main heat flow peak tends to be delayed and less intensive. As is evident from Fig. 3a, the presence of SB results in a slight retardation effect on the hydration of CSA cement. For instance, at 5% of SB dispersion addition, the maxima of the heat flow is shifted from 108 to 125 min, and the heat flow value is decreased from 26.76 to 24.79 mW g^{-1}. When the content of SB increases, the retardation effect is much more significant. With addition of 20% SB in CSA cement paste, the second heat flow peak occurs at 140 min with heat flow of 24.53 mW g^{-1}, which is delayed 15 min and decreased 1.07 mW g^{-1} in comparison with that of CSA cement paste with addition of 5% SB dispersion. The explanation can be given that along with the hydration, SB dispersion delays the formation of ettringite by covering the surface of cement grains. However, the effect of SB dispersion on the third heat flow peak seems to be not consistent with that on the second one. In this stage, the SB dispersion delays the heat flow evolution firstly (from 18 to 21 h) at addition of 5% and then starts to accelerate it to an earlier time with the dosage increasing.

The cumulative heat generation of CSA cement paste with and without SB dispersion is exhibited in Fig. 3b, in which SB dispersion decreases the heat generation within the initial 3 h; the more SB is added, the less heat is released. As described above, this phenomenon is mainly ascribed to the delayed hydration of CSA cement by SB dispersion, which causes less formation of ettringite. Afterward, the heat generation from SB-modified CSA cement paste becomes higher than that from the control paste, which means the hydration of CSA cement is accelerated in this period. Along with the hydration, the hydration heat of SB-modified CSA cement paste seems to be quite similar as each other after 40 h, which indicates that the hydration extent tends to be consistent with each other.

The influence of SA on the hydration heat of CSA cement paste within 72 h is shown in Fig. 4. Figure 4a shows that SA dispersion significantly delays the occurring time of the second heat flow peak. The second peak of CSA cement paste with 5% SA dispersion is prolonged from 108 to 128 min. When the addition of SA dispersion increases to 20%, the heat flow peak appears at 194 min, which is much longer than that of the control. The heat flow value in this stage is obviously decreased. For instance, the heat

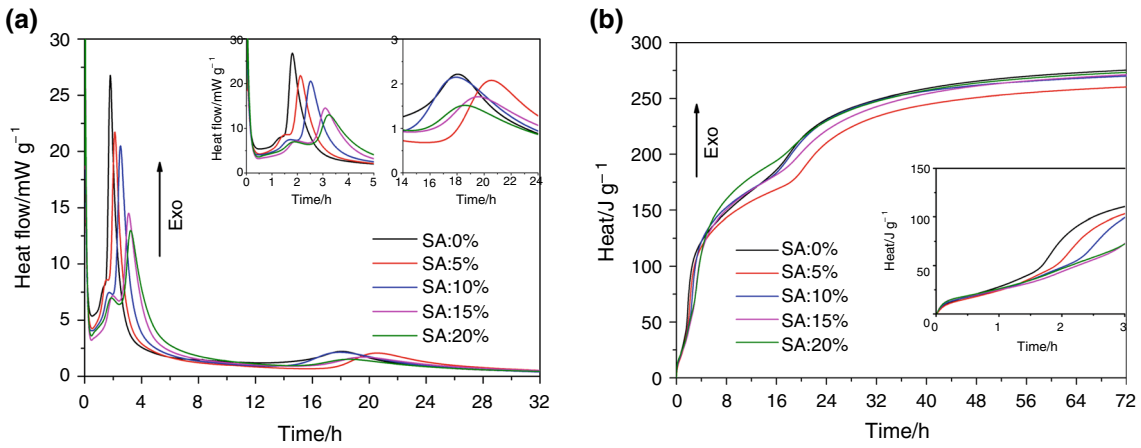

Fig. 4 Hydration heat characteristics of CSA cement pastes modified with SA dispersion: **a** heat flow and **b** cumulative heat

flow of CSA cement paste with 20% of SA dispersion is 12.97 mW g^{-1}, which accounts for 48% of heat flow of the control. It is also found that the shoulder within this period becomes obvious when the amount of SA increases. This is mainly ascribed to the formation of dihydrate due to delayed initial hydration, which can be confirmed by XRD analysis in the following sections.

The heat generation of SA-modified CSA cement paste is displayed in Fig. 4b. It is found that the cumulative heat of CSA cement paste is reduced by SA within the initial 5 h, and the CSA cement with addition of 15% of SA dispersion owns similar value as that with addition of 20% SA. Afterward, the heat is released sharply for those with SA dispersion, and the CSA cement paste with 20% of SA shows the highest heat generation between 5 and 17 h. With time evolution, the hydration heat of CSA cement with SA dispersion tends to be close to that of the control paste although CSA cement paste with 5% of SA shows the lowest heat value.

The hydration heat flow of PA-modified CSA cement paste is shown in Fig. 5a. PA displays the similar effect on the second maximum peak as SA, but more significantly. When the addition of PA dispersion is 20%, the heat flow maximum occurs at 267 min, which is much longer than that of the control paste. The heat flow value of CSA cement paste is also sharply decreased by PA. The higher amount of PA dispersion is dosed, the less heat flow value is generated. The heat flow of CSA cement paste with addition of 20% PA is 9.15 mW g^{-1}, which is 34% of that from the control paste. The influence of PA dispersion on the third heat flow peak is different from SB and SA dispersion. PA dispersion significantly shortens the occurring time of the third peak while increases the heat flow value. Figure 5a shows that the addition of 10% PA performs the shortest occurring time of the third peak and with the highest heat flow value, which indicates that CSA cement paste with 10% of PA dispersion shows the best acceleration during this stage.

Figure 5b illustrates the effect of PA on the total heat development of CSA cement paste. The heat generation of CSA cement paste within the initial 3 h is decreased when with PA dispersion, and then, the heat releasing speed

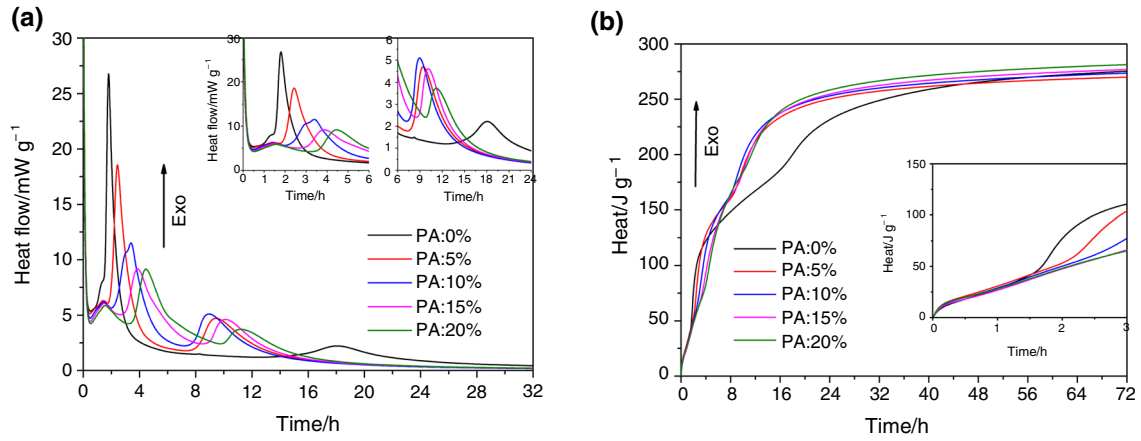

Fig. 5 Hydration heat characteristics of CSA cement pastes modified with PA dispersion: **a** heat flow and **b** cumulative heat

reduces in the following periods when PA increases. The CSA cement paste with 10% PA shows the highest heat value when the hydration time is between 8 h and 16 h. Afterward, the higher amount of PA dispersion is added in CSA cement paste, the higher heat value is generated, and the CSA cement paste with addition of 20% PA shows the highest heat value.

The comparison analysis on the influence of three polymer dispersions on the heat flow peaks of CSA cement paste is conducted. Generally, the addition of polymer dispersions in CSA cement pastes prolongs the occurring time (Fig. 6a) and decreases the heat flow value (Fig. 6b) of the second maximum peak; however, the extent of the impact varies with the types of polymer dispersions. It is seen that PA dispersion exhibits the biggest retardation effect while SB shows the lowest impact on the hydration of CSA cement. The influence of polymer dispersions shows the different trends on the third heat flow maximum (Fig. 6c, d). PA dispersion significantly shortens the third peak appearing time and increases the heat flow value. The addition of 10% PA dispersion in CSA cement paste shows the biggest influences which has been described in above. CSA cement paste with 5% of SB dispersion shows the delayed peak time; afterward, the peak time reduces with SB dispersion increasing. SA dispersion shows the similar impact on the third peak time as SB, but the extent is much lower. Both SB and SA decrease the heat flow value, and SA displays the bigger effect when the content of polymer dispersion is more than 10%.

The hydration heat of CSA cement paste with addition of 10% of various polymer dispersions is exhibited in Fig. 7. PA dispersion demonstrates the highest heat flow within 90 min, although it is still a little bit lower than that from the control paste. Afterward, PA dispersion starts to suppress the heat generation and shows the lowest heat value within 5 h compared to other polymers. During this period, SB dispersion promotes to release the highest heat. The hydration kinetics of CSA cement paste are accelerated by PA dispersion after 5 h, and it performs the highest heat value for the following periods. In order to better understand the effect of polymer dispersions on the hydration mechanism of CSA cement paste, the further investigation by use of setting time,

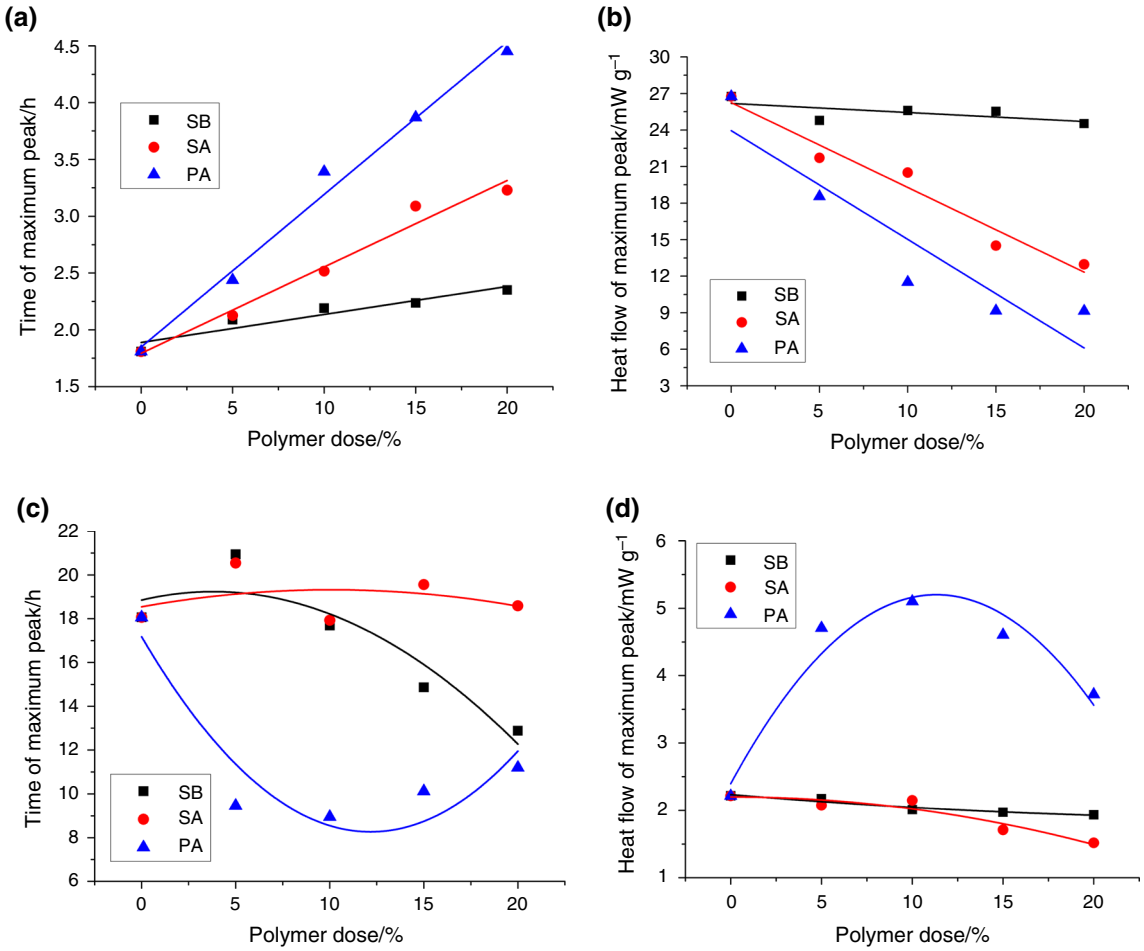

Fig. 6 Comparison analysis of hydration heat: **a** occurring time of the second peak; **b** heat flow of the second peak; **c** occurring time of the third peak; **d** heat flow of the third peak

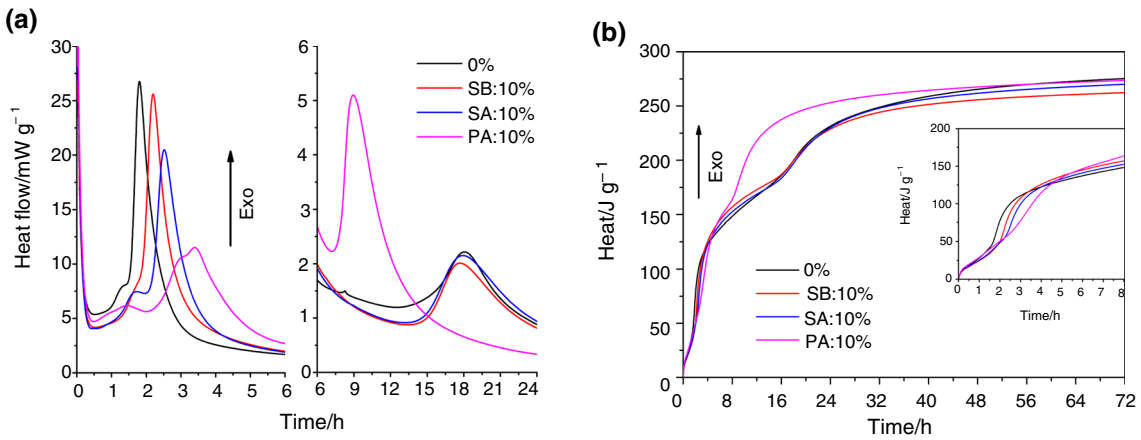

Fig. 7 Comparison of hydration heat development of CSA cement pastes modified with various polymer dispersions at 10% dosage: **a** heat flow and **b** cumulative heat

XRD and TGA was conducted and the results have been discussed in the following sections.

Setting time

The setting times of polymer-modified CSA cement pastes, as listed in Table 4, are well consistent with calorimetric results that the addition of polymer dispersions shows the retardation effect on CSA cement paste. The initial and final setting times of CSA control paste are 46 min and 62 min, respectively. Addition of 10% SB dispersion in CSA cement paste demonstrates the longest setting time (101 min and 110 min) while addition of 10% PA dispersion has the shortest setting time (72 min and 97 min). As described in above, the PA-modified CSA cement paste performs the highest heat flow as well as total heat within 90 min, indicating the highest reactivity among these three polymer-modified CSA cement pastes; therefore, the shortest setting time is achieved.

XRD analysis

XRD patterns of CSA cement pastes modified with 10% polymer dispersions at various curing ages are displayed in Fig. 8. Figure 8a shows that the dominant hydration product of CSA cement is ettringite, which is formed via the reaction according to Eq. (1). The formation of ettringite is gradually increased with hydration time prolongation. Besides of ettringite, hemicarboaluminate (Hc) can be also detected at 1 day and reaches the highest amount at 3 days. The formation of Hc is mainly due to the presence of carbonate mineral (dolomite) in CSA cement [58].

Table 4 Setting time of CSA cement pastes modified with various polymer dispersions

Polymer content	Setting time/min	
	Initial setting time	Final setting time
0%	46	62
SB: 10%	101	110
SA: 10%	98	105
PA: 10%	72	97

The similar hydration products are generated in SB-modified CSA cement pastes although the extent is different at each curing age. Figure 8b shows that the addition of SB dispersion in CSA cement paste significantly decreases the formation of ettringite at 1 h, which indicates a remarkable retardation effect from SB dispersion on the hydration kinetics of CSA cement within 1 h. The peak of dihydrate is detectable at 1 h; it is formed at this stage due to the hydration of anhydrate according to Eq. (3). The addition of SB delays the hydration reaction between anhydrite and ye'elimite at the initial stage; thus, the anhydrite starts to react with water to form dihydrate firstly. However, the generation of ettringite is boosted at 2 h. Meanwhile, the peak of Hc is not obvious which means SB is helpful to inhibit the formation of Hc in CSA cement paste.

$$C\bar{a}S\bar{O}_4 + 2H_2O \rightarrow C\bar{a}S\bar{O}_4 \cdot 2H_2O \quad (3)$$

Similar phenomenon is observed from Fig. 8c and d that the formation of ettringite is delayed within 1 h and then boosted at 2 h. However, Hc can be observed after 1 day and reaches the highest amount at 3 days. It can be concluded that the addition of SA and PA dispersion in CSA cement paste shows less inhibition on the formation of Hc compared with SB dispersion.

The effect of polymer dispersions on the formation of hydration products in CSA cement paste at 1 h and 3 days is further discussed. Figure 9a shows that polymer

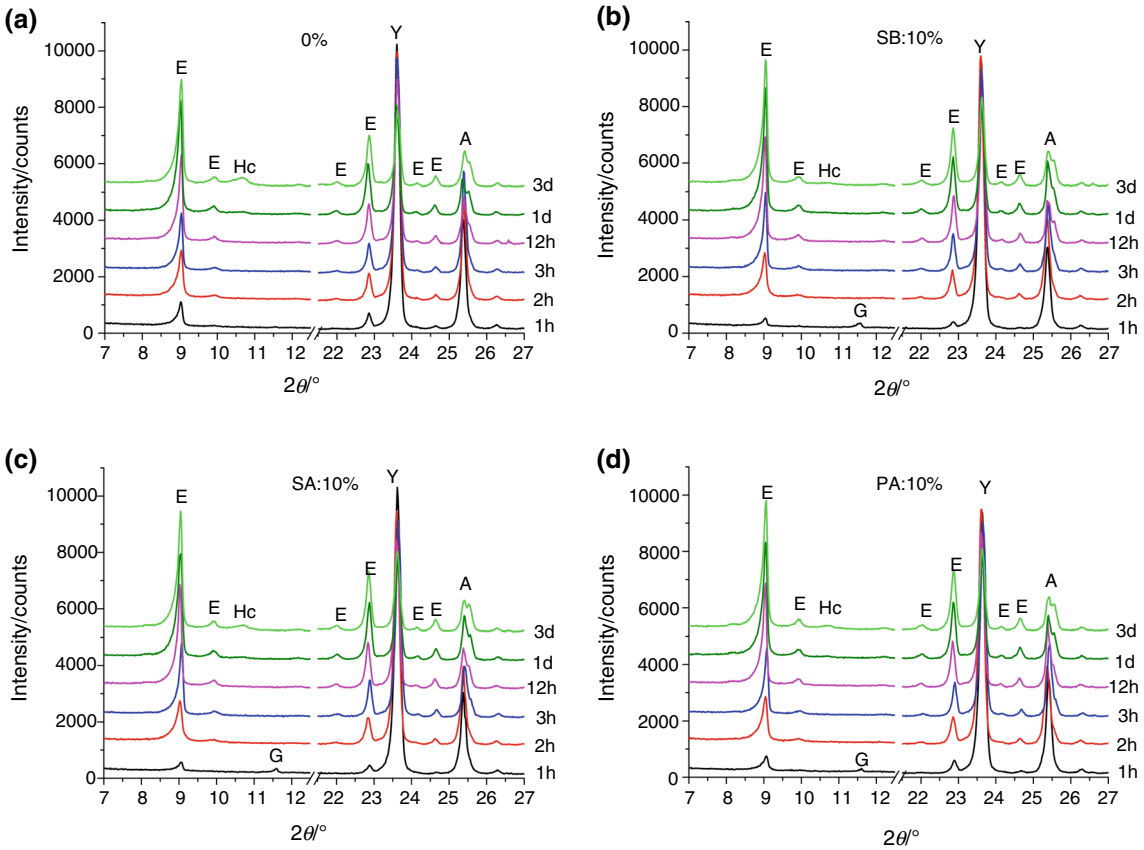

Fig. 8 XRD patterns of CSA cement pastes with addition of **a** 0%, **b** SB: 10%, **c** SA: 10% and **d** PA: 10% at 1 h, 2 h, 3 h, 12 h, 1 day and 3 days (Y: ye'elimite, A: anhydrite, E: ettringite, Hc: hemicarboaluminate, G: dihydrate)

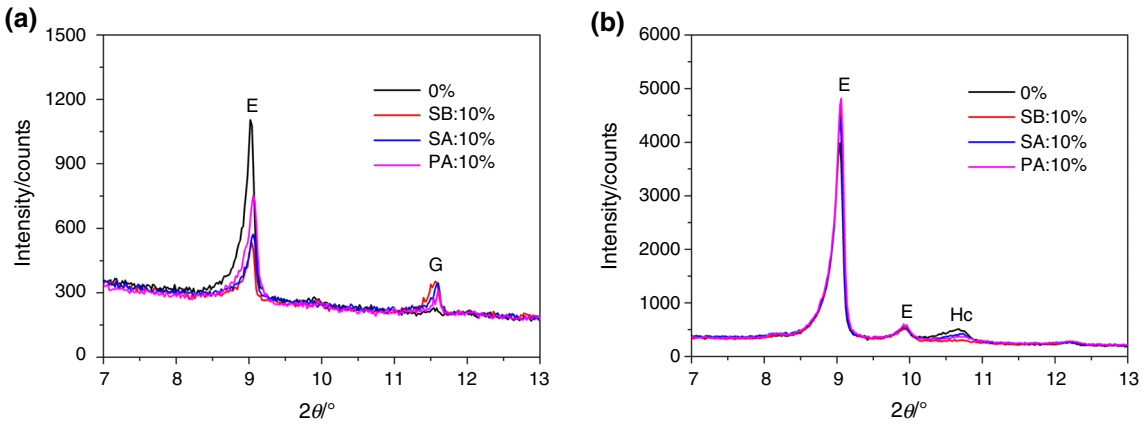

Fig. 9 XRD patterns of CSA cement pastes with addition of 10% polymer dispersion at **a** 1 h and **b** 3 days (E: ettringite, Hc: hemicarboaluminate, G: dihydrate)

dispersions significantly decrease the formation of ettringite at 1 h. SB and SA dispersions perform higher inhibitory effect on the formation of ettringite while PA dispersion shows less inhibitory effect. Meanwhile, the formation of dihydrate is observed in polymer-modified CSA cement pastes. When curing time reaches 3 days, the ettringite generated from polymer-modified CSA cement paste is higher than that from CSA control paste (see Fig. 9b); meanwhile, the formation of Hc is well suppressed by polymer dispersion and SB demonstrates the best effect among three polymers.

The generation of ettringite is accompanied by the consumption of ye'elimite and anhydrite, which are the main phases of CSA cement minerals. The relationship

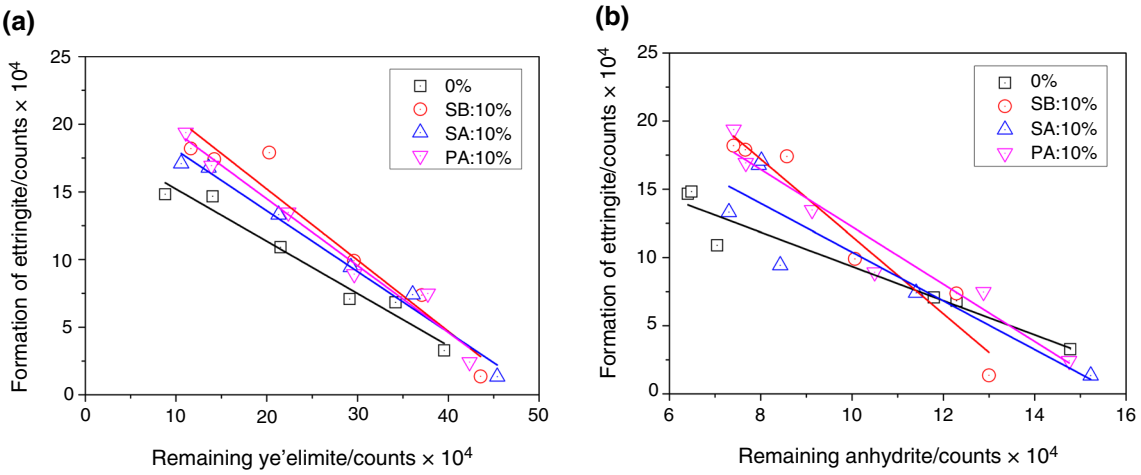

Fig. 10 Relationship between the formation of ettringite and **a** remaining ye'elimite, **b** remaining anhydrite

between the formation of ettringite and the residue of ye'elimite as well as anhydrite is plotted in Fig. 10. It is seen that the higher content of ettringite is generated, the less amount of ye'elimite and anhydrite is left after hydration. However, different polymer dispersions show different degrees of negative correlation; the detail linear correlation equation is listed in Table 5. Generally, polymer-modified CSA cement paste demonstrates higher conversion rate to ettringite than CSA control paste, and SB dispersion performs the highest acceleration while SA shows the lowest.

Thermal analysis

The TG/DTG curves of CSA cement pastes with and without polymer dispersions at various hydration times of 1 h, 2 h, 3 h, 12 h, 1 day and 3 days are shown in Fig. 11. Figure 11a shows that there are two main peaks appearing on DTG curves of the control CSA cement pastes. The main derivative peak shown between 100 and 150 °C attributes to the water removal from ettringite, which gradually increases with hydration time prolongation. The second peak shown at around 260 °C mainly corresponds to the structure water loss from AH_3 gel. The amount of AH_3 increases with hydration time prolongation from 1 h to 3 days. The hydrate Hc is not remarkable in DTG plots, which is attributed to their minor amount.

The addition of polymer dispersions in CSA cement paste significantly decreases the formation of ettringite in the early stage. Figure 11b–d shows that the weak peak of ettringite is detectable at hydration time of 1 h in comparison with CSA control paste (see Fig. 11a). However, the peak of ettringite in Fig. 11d is much more remarkable than that in Fig. 11b and c, indicating the less delay effect on ettringite generation from PA dispersion. Another peak at around 125 °C corresponds to the formation of calcium sulfate dihydrate, which is due to the reaction between anhydrite and water according to Eq. (3), as described in above section. The derivative peaks of ettringite from polymer-modified CSA cement become much more remarkable than those from control paste at and after 2 h, indicating acceleration effect on the formation of ettringite from polymers. This result is well consistent with that from XRD analysis.

Meanwhile, the peaks corresponding to AH_3 are shown in Fig. 11. The formation of AH_3 in this study is mainly ascribed to the hydration reaction of ye'elimite, anhydrite and water, according to Eqs. (1) and (2). Generally, the amount of AH_3 increases with hydration time prolongation, and polymer dispersion shows limit impact on it. It is also found that the addition of polymer dispersions in CSA cement paste benefits to reduce the formation of Hc, which could be detected at around 180 °C in the DTG curves.

Table 5 Correlation analysis between the formation of ettrintite and the residue of ye'elimite and anhydrite

	Linearly fitting of ettringite versus ye'elimite	Linearly fitting of ettringite versus anhydrite
0%	$y = 19.069–0.386x$, $R^2 = 0.959$	$y = 21.883–1.253x$, $R^2 = 0.925$
SB: 10%	$y = 25.726–0.526x$, $R^2 = 0.926$	$y = 39.885–2.834x$, $R^2 = 0.926$
SA: 10%	$y = 22.582–0.449x$, $R^2 = 0.983$	$y = 28.257–1.786x$, $R^2 = 0.759$
PA: 10%	$y = 24.371–0.494x$, $R^2 = 0.967$	$y = 33.276–2.102x$, $R^2 = 0.937$

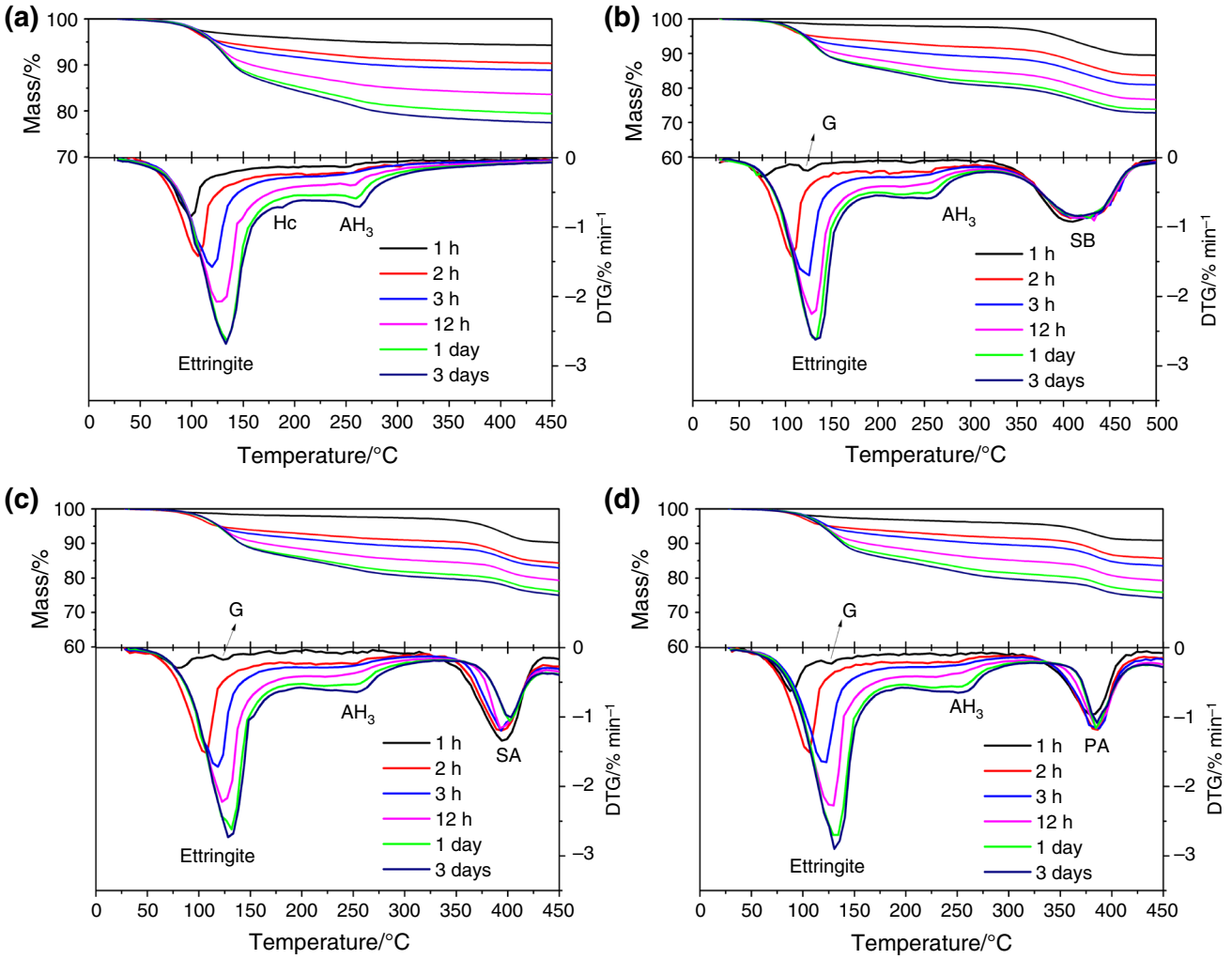

Fig. 11 TG/DTG curves of CSA cement pastes with addition of **a** 0%, **b** SB: 10%, **c** SA: 10% and **d** PA: 10% (Hc: hemicarboaluminate, AH_3: aluminum hydroxide, G: dihydrate)

Hydration process

The hydration process is revealed by phase assemblage evolution based on the results from XRD and TG analysis. The minerals content of ye'elimite and anhydrite is roughly estimated based on XRD intensity according to references [50, 59]. The amount of ettringite, AH_3 and Hc and pore solution are calculated from TGA results. Figure 12 shows that the hydration process of polymer-modified CSA cement paste is quite similar as that of control CSA cement paste while some big difference can be seen at the hydration time of 1 h. In this stage, the formation of ettringite from CSA cement paste is significantly delayed by polymer dispersions. The addition of PA dispersion shows the least effect, which can be reflected by the highest formation of ettringite among polymer-modified CSA cement pastes. Meanwhile, the formation of calcium sulfate dihydrate can be also found due to the reaction between anhydrite and water in polymer-modified CSA cement pastes. The hydration degree of CSA cement is caught up by that of polymer-modified CSA cement when hydration time comes to 2 h.

The effect of polymer dispersions on the hydration of CSA cement can be divided into two stages based on above results: the very early retardation period and later acceleration period. The incorporation of polymer dispersions prolongs the setting time of CSA cement paste (Table 4) due to its initial retardation effect on CSA cement hydration, which is well consistent with previous studies for polymer-modified Portland cement [20, 23, 25, 27, 29]. The calorimetry measurement is very suitable to be employed to monitor the initial hydration of CSA cement modified with polymer dispersions. It is found from calorimetry analysis that the retardation effect from polymer dispersions can be mainly ascribed to two reasons: depressing the hydration heat flow rate and decreasing the cumulative heat volume (Fig. 7). The further explanation on this effect can be given through electrostatic force due to the adsorption of polymer particles onto cement grains

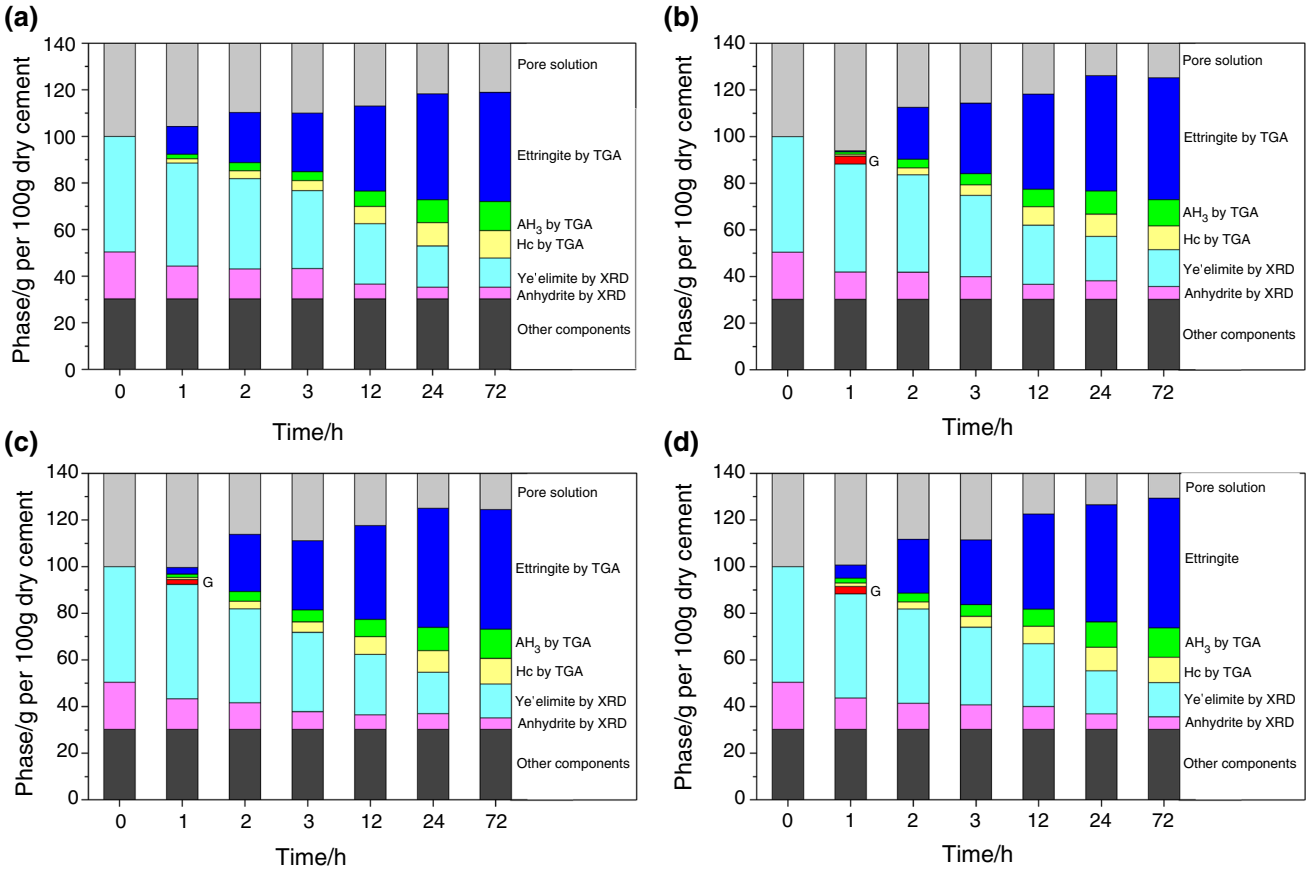

Fig. 12 Hydration process of CSA cement with addition of **a** 0%, **b** SB: 10%, **c** SA: 10% and **d** PA: 10% (AH_3: aluminum hydroxide, Hc: hemicarboaluminate, G: dihydrate)

[14, 17, 23, 34]. The polymer dispersions used in this experiment are modified by anionic surfactants during synthesis process; in this case, they undertake negative charges within their own system. Different from polymer dispersions, the cement mineral grains take positive charges, which tend to be covered with polymer particles due to the ionic bonding effect. The polymer coverage layer reduces the interaction between cement minerals and water and finally inhibits the early hydration [14, 23, 31].

As a consequence of delayed initial hydration of polymer-modified CSA cement, the formation of ettringite at 1 h is significantly retarded while small amount of dihydrate was detected. This result is well confirmed by XRD and TGA results. As the hydration proceeds, the polymer coverage layer is broken through by the initial hydrates; accordingly, the hydration rate starts to be accelerated, and a slight more hydrates comprising ettringite and AH_3 are formed. Furthermore, the increased space given by the longer distance between cement particles due to electrostatic force from negative charged polymer particles contributes to its increasing effect.

Generally, the used three polymer dispersions perform the close effect on the early hydration of CSA cement, although the difference among the hydration processes of these various polymer-modified CSA cement pastes can be seen. PA-modified CSA cement paste demonstrates the strongest retardation effect on the second hydration heat flow peak while SA shows the lowest among three polymer-modified CSA cement pastes (Fig. 6). However, the opposite phenomena are shown in Fig. 7 that the CSA cement paste modified with PA has the highest heat flow as well as the highest cumulative heat within 90 min, which is mainly due to the biggest formation of ettringite. The variation between these three polymer-modified CSA cement pastes mainly exists in this initial stage, and the hydration processes of polymer-modified CSA cement pastes are very consistent with the control paste after 2 days.

Conclusions

The effect of polymer dispersions on the early hydration of CSA cement was investigated. Three polymer dispersions (SB, SA and PA) with five different ratios (0, 5, 10, 15 and 20%) to CSA cement were added into CSA cement pastes

at a constant water-to-cement ratio of 0.4. The main conclusions are summarized as follows:

1. Generally, polymer-modified CSA cement pastes perform similar hydration evolution as that of the control paste, although the initial stage was highly influenced. The addition of polymer dispersions significantly retards the initial hydration of CSA cement, especially within 1 h; thus, the setting time is prolonged. The results from XRD and TGA at 1 h reveal that the generation of ettringite is strongly delayed while calcium sulfate dihydrate is formed in polymer-modified CSA cement paste.
2. The ettringite content generated from control CSA cement paste is exceeded by that from polymer-modified CSA cement pastes at and after 2 h. PA-modified CSA cement paste demonstrates the highest amount of ettringite among these polymer-modified CSA cement pastes.
3. The higher generation of ettringite is accompanied with bigger depletion of ye'elimite and anhydrite. Generally, polymer-modified CSA cement paste demonstrates higher conversion rate to ettringite than control CSA cement paste. Among these three polymer-modified CSA cement pastes, SB dispersion performs the highest acceleration while SA shows the lowest.
4. The addition of polymer dispersions shows good inhibition effect on the formation of hemicarboaluminate.

Acknowledgements The authors acknowledge the financial support by the National Natural Science Foundation of China (Grant Nos. 51572196 and 51872203) and Sino-German Center for Research Promotion (Grant No. GZ 1290).

References

1. Wang R, Wang P. Function of styrene-acrylic ester copolymer latex in cement mortar. Mater Struct. 2010;43(4):443–51.
2. Eren F, Godek E, Keskinates M, Tosun-Felekoglu K, Felekoglu B. Effects of latex modification on fresh state consistency, short term strength and long term transport properties of cement mortars. Constr Build Mater. 2017;133:226–33.
3. Bauereggera S, Perellob M, Plank J. On the role of colloidal crystal-like domains in the film forming process of a carboxylated styrene-butadiene latex copolymer. Prog Org Coat. 2014;77:685–90.
4. Assaad JJ. Development and use of polymer-modified cement for adhesive and repair applications. Constr Build Mater. 2018;163:139–48.
5. Rossignolo JA, Agnesini MVC. Mechanical properties of polymer-modified lightweight aggregate concrete. Cem Concrete Res. 2002;32(3):329–34.
6. Reis JML. Mechanical characterization of polymer mortars exposed to degradation solutions. Constr Build Mater. 2009;23(11):3328–31.
7. Ramli M, Tabassi AA. Effects of different curing regimes on engineering properties of polymer-modified mortar. J Mater Civ Eng. 2012;24(4):468–78.
8. Rossignolo JA, Agnesini MVC. Durability of polymer-modified lightweight aggregate concrete. Cem Concrete Compos. 2004;26(4):375–80.
9. Shaker FA, El-Dieb AS, Reda MM. Durability of styrene-butadiene latex modified concrete. Cem Concrete Res. 1997;27(5):711–20.
10. Vo ML, Plank J. Evaluation of natural rubber latex as film forming additive in cementitious mortar. Constr Build Mater. 2018;169:93–9.
11. Jiang CH, Huang SS, Gao P, Chen D. Experimental study on the bond and durability properties of mortar incorporating polyacrylic ester and silica fume. Adv Cem Res. 2018;30(2):56–65.
12. Rozenbaum O, Pellenq RJM, Van Damme H. An experimental and mesoscopic lattice simulation study of styrene-butadiene latex-cement composites properties. Mater Struct. 2005;38(278):467–78.
13. Plank J, Gretz M. Study on the interaction between anionic and cationic latex particles and Portland cement. Colloid Surf A Physicochem Eng Asp. 2008;330:227–33.
14. Lu Z, Kong X, Zhang Q, Cai Y, Zhang Y, Wang Z, et al. Influences of styrene-acrylate latexes on cement hydration in oil well cement system at different temperatures. Colloid Surf A Physicochem Eng Asp. 2016;507:46–57.
15. Lu Z, Kong X, Zhang C, Cai Y, Zhang Q, Zhang Y. Effect of polymer latexes with varied glass transition temperature on cement hydration. J Appl Polym Sci. 2017;134(36):45264.
16. Vitorino FC, Filho RDT, Dweck J. Hydration at early ages of styrene-butadiene copolymers cementitious systems. J Therm Anal Calorim. 2018;131(2):1041–54.
17. Fan J, Guo J, Chen D, Hu M, Cao L, Xu Y, et al. Effects of submicron core-shell latexes with different functional groups on the adsorption and cement hydration. Constr Build Mater. 2018;183:127–38.
18. Kong X, Pakusch J, Jansen D, Emmerling S, Neubauer J, Goetz-Neuhoeffer F. Effect of polymer latexes with cleaned serum on the phase development of hydrating cement pastes. Cem Concrete Res. 2016;84:30–40.
19. Wang R, Yao L, Wang P. Mechanism analysis and effect of styrene-acrylate copolymer powder on cement hydrates. Constr Build Mater. 2013;41:538–44.
20. Han D, Chen W, Zhong S. Physical retardation mechanism of latex polymer on the early hydration of cement. Adv Cem Res. 2018;30(3):113–22.
21. Fichet RO, Gauthier C, Clamen G, Boch P. Micorstructure aspects in a polymer modified cement. Cem Concrete Res. 1998;28(12):1687–93.
22. Su Z, Bijen JMJM, Larbi JA. Influence of polymer modification on the hydration of portland cement. Cem Concrete Res. 1991;21:535–44.
23. Kong XM, Emmerling S, Pakusch J, Rueckel M, Nieberle J. Retardation effect of styrene-acrylate copolymer latexes on cement hydration. Cem Concrete Res. 2015;75:23–41.
24. Gao JM, Qian CX, Wang B, Morino K. Experimental study on properties of polymer-modified cement mortars with silica fume. Cem Concrete Res. 2002;32(1):41–5.
25. Wang M, Wang RM, Zheng SR, Farhan S, Yao H, Jiang H. Research on the chemical mechanism in the polyacrylate latex modified cement system. Cem Concrete Res. 2015;76:62–9.
26. Ohama Y. Principle of latex modification and some typical properties of latex-modified mortars and concretes. ACI Mater J. 1987;84(6):511–8.

27. Betioli AM, Filho JH, Cincotto MA, Gleize PJP, Pileggi RG. Chemical interaction between EVA and Portland cement hydration at early-age. Constr Build Mater. 2009;23:3332–6.
28. Chandra S, Flodin P. Interactions of polymers and organic admixtures on portland cement hydration. Cem Concrete Res. 1987;17(6):875–90.
29. Baueregger S, Perello M, Plank J. Influence of carboxylated styrene–butadiene latex copolymer on Portland cement hydration. Cem Concrete Compos. 2015;63:42–50.
30. Abo-El-Enein SA, Hanafi S, El-Hosiny FI, El-Said HM, El-Mosallamy ES, Amin MS. Effect of some acrylate-poly(ethylene glycol) copolymers as superplasticizers on the mechanical and surface properties of Portland cement pastes. Adsorpt Sci Technol. 2005;23(3):245–54.
31. Zhang G, Wang Y, Wang P, Xu L. Calorimetric study on the influence of redispersible E/VC/VL terpolymer on the early hydration of Portland cement. J Therm Anal Calorim. 2016;124:1229–41.
32. Jin Y, Stephan D. Hydration kinetics of Portland cement in the presence of vinyl acetate ethylene latex stabilized with polyvinyl alcohol. J Mater Sci. 2018;53:417–30.
33. Baueregger S, Perello M, Plank J. Impact of carboxylated styrene–butadiene copolymer on the hydration kinetics of OPC and OPC/CAC/AH: the effect of Ca^{2+} sequestration from pore solution. Cem Concrete Res. 2015;72:184–9.
34. Lu Z, Kong X, Zhang C, Xing F, Cai Y, Jiang L, et al. Effect of surface modification of colloidal particles in polymer latexes on cement hydration. Constr Build Mater. 2017;155(30):1147–57.
35. Wang R, Li X, Wang P. Influence of polymer on cement hydration in SBR-modified cement pastes. Cem Concrete Res. 2006;36(9):1744–51.
36. Wang R, Wang P. Formation of hydrates of calcium aluminates in cement pastes with different dosages of SBR powder. Constr Build Mater. 2011;25:736–41.
37. Glasser FP, Zhang L. High-performance cement matrices based on calcium sulfoaluminate–belite compositions. Cem Concrete Res. 2001;31(12):1881–6.
38. Li HX, Agrawal DK, Cheng JP, Silsbee MR. Microwave sintering of sulphoaluminate cement with utility wastes. Cem Concrete Res. 2001;31(9):1257–61.
39. Zhang Y, Chang J, Ji J. AH_3 phase in the hydration product system of AFt-AFm-AH_3 in calcium sulfoaluminate cements: a microstructural study. Constr Build Mater. 2018;167:587–96.
40. Shen Y, Chen X, Zhang W, Li X. Effect of ternesite on the hydration and properties of calcium sulfoaluminate cement. J Therm Anal Calorim. 2019;136(2):687–95.
41. Shen Y, Li X, Chen X, Zhang W, Yang D. Synthesis and calorimetric study of hydration behavior of sulfate-rich belite sulfoaluminate cements with different phase compositions. J Therm Anal Calorim. 2018;133(3):1281–9.
42. Winnefeld F, Barlag S. Calorimetric and thermogravimetric study on the influence of calcium sulfate on the hydration of ye'elimite. J Therm Anal Calorim. 2010;101(3):949–57.
43. Wang YM, Su MZ, Zang L. Sulphoaluminate cement. Beijing: Beijing Industry University Press; 1999 **(in Chinese)**.
44. Berger S, Cournes CCD, Le Bescop P, Damidot D. Influence of a thermal cycle at early age on the hydration of calcium sulphoaluminate cements with variable gypsum contents. Cem Concrete Res. 2011;41(2):149–60.
45. Pelletier-Chaignat L, Winnefeld F, Lothenbach B, Muller CJ. Beneficial use of limestone filler with calcium sulphoaluminate cement. Constr Build Mater. 2012;26(1):619–27.
46. Hargis CW, Telesca A, Monteiro PJM. Calcium sulfoaluminate (ye'elimite) hydration in the presence of gypsum, calcite, and vaterite. Cem Concrete Res. 2014;65:15–20.
47. Garcia-Mate M, De la Torre AG, Leon-Reina L, Losilla ER, Aranda MAG, Santacruz I. Effect of calcium sulfate source on the hydration of calcium sulfoaluminate eco-cement. Cem Concrete Compos. 2015;55:53–61.
48. Xu L, Liu S, Li N, Peng Y, Wu K, Wang P. Retardation effect of elevated temperature on the setting of calcium sulfoaluminate cement clinker. Constr Build Mater. 2018;178:112–9.
49. Zhang Y, Zhang Z, Li W, Wang H, Shen X. Welan gum retards the hydration of calcium sulfoaluminate. J Therm Anal Calorim. 2017;130(2):899–908.
50. Winnefeld F, Lothenbach B. Hydration of calcium sulfoaluminate cements: experimental findings and thermodynamic modelling. Cem Concrete Res. 2010;40(8):1239–47.
51. Li L, Wang R, Lu Q. Influence of polymer latex on the setting time, mechanical properties and durability of calcium sulfoaluminate cement mortar. Constr Build Mater. 2018;169:911–22.
52. ISO 9597:2008 Cement: test methods—determination of setting time and soundness.
53. Huang YB, Qian JS, Liang J, Liu N, Li FL, Shen Y. Characterization and calorimetric study of early-age hydration behaviors of synthetic ye'elimite doped with the impurities in phosphogypsum. J Therm Anal Calorim. 2016;123(2):1545–53.
54. Winnefeld F, Barlag S. Influence of calcium sulfate and calcium hydroxide on the hydration of calcium sulfoaluminate clinker. ZKG Int. 2009;62(12):42–53.
55. Zhang L, Glasser FP. Hydration of calcium sulfoaluminate cement at less than 24 h. Adv Cem Res. 2002;14(4):141–55.
56. Jansen D, Spies A, Neubauer J, Ectors D, Goetz-Neunhoeffer F. Studies on the early hydration of two modifications of ye'elimite with gypsum. Cem Concrete Res. 2017;91:106–16.
57. Zhang G, He R, Lu X, Wang P. Early hydration of calcium sulfoaluminate cement in the presence of hydroxyethyl methyl cellulose. J Therm Anal Calorim. 2018;134(3):1429–38.
58. Zajac M, Bremseth SK, Whitehead M, Ben HM. Effect of $CaMg(CO_3)_2$ on hydrate assemblages and mechanical properties of hydrated cement pastes at 40 °C and 60 °C. Cem Concrete Res. 2014;65:21–9.
59. Li N, Xu L, Wang R, Li L, Wang P. Experimental study of calcium sulfoaluminate cement-based self-leveling compound exposed to various temperatures and moisture conditions: hydration mechanism and mortar properties. Cem Concrete Res. 2018;108:103–15.